Angle-Resolved Photoelectron Spectrometer for the Use of Surface Study of Solids

Angle-Resolved Photoelectron Spectrometer for the Use of Surface Study of Solids

Shoji SUZUKI, Kenji FURUSAWA, Masaaki TERASAWA, Midori YOSHIDA and Takasi SAGAWA

Department of Physics, Faculty of Science, Tohoku University, Sendai 980, Japan

(Received April 15, 1980)

An angle-resolved photoelectron spectrometer constructed recently in our laboratory is described in detail, which comprises mainly from an electron energy analyser movable in situ from the outside of an ultra-high-vacuum (UHV) chamber, an UV light source and a sample manipulator. An ion-pump system is used to evacuate the chamber up to better vaccum than 10^{-10}Torr. Several other auxiliary equipments such as LEED, RHEED and/or RMEED apparatus, Ar^+ ion-bombardment and/or sample cleaving systems, a mass spectrometer and a gas inlet system are installed in the chamber.

Some obtained results by the apparatus are shown as the typical examples in order to demonstrate the high performance attained.

Keywords:Angle-Resolved Photoemission, Surface

§1. Introduction

In recent years, it has been known well that the angle-resolved photoelectron spectroscopy (ARPES) is a powerful tool to investigate the electronic structures and atomic arrangements in the clean and gas-adsorbed surfaces of solids[1] and further to map out the bulk band dispersions, E vs $\vec{k}$, directly[2]. In the ARPES measurements, the kinetic energies of photoelectrons are observed within a narrow angular cone under continuous variation of the one of parameters to be appeared, such as an incidence angle α of light, a photon energy $\hbar\omega$ and a polar angle θ and an azimuthal angle ϕ of photoelectrons. A polarization direction s or p of incident light with respect to the surface and an index (hkl) of the surface net plane in a single crystal sample are also the important parameters to be determined before measurements. All parameters appeared in the ARPES are shown schematically in Fig. 1 to see these situations. A spin polarization of photoelectrons is observed sometimes in addition for magnetic materials[3], but this is not the case in this report. In the cases, where the rare-gas discharge lamp is used as a light source, the photon energy $\hbar\omega$ can not be varied continuously and usually the polar angle (θ) or light incidence-angle (α) dependence is observed within a fixed

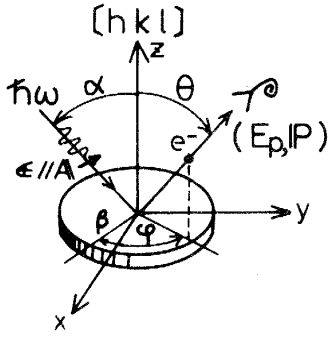

Fig.1. Various parameters appeared in the ARPES.

azimuthal plane for the constant α or θ, correspondingly. The α dependence is somewhat equivalent to the dependence on the polarization direction of light. The $\hbar\omega$ dependences can be obtained nicely using by the synchrotron radiation[4], which has many other excellent characteristics for ARPES in its high degrees of polarization, cleanliness, high intensity, highly collimated nature of the beam, short pulse nature in the time structure and so on. On the other hand, the azimuthal dependence is measured usually for the cases of core electrons or valence electrons limited within narrow energy range, mainly for the purpose of the determination of atomic geometries on the surface, which gives a so-called flower pattern on the 360° diagram in general[5]. Similar informations can be obtained also from the $\hbar\omega$ dependences[6]. These features are caused mainly by the final-state inferference effects and then somewhat analogous to the EXAFS.

In the ARPES, the momentum component parallel to the surface of photoelectron is conserved in both sides of the surface, while the perpendicular component to the surface is not conserved in general due to refraction. Therefore, the inner momentum of photoelectron can not be known directly from the outer momentum as explained in Fig.2, where the inner and outer momenta are denoted as $\vec{k}$ and $\vec{p}$, respectively. On the left part in Fig.2, the energy conservation relation is shown for convenience. The direct interband transition model (DTM) which is most dominant in the optical absorption processes in the bulk as known well is not necesarrily obvious in the photoemission processes, because the photoelectron has a short mean free path $l(E)$ in the bulk. This situation can be represented explicitly by introducing a complex crystal momentum along normal direction to the surface, as $k_\perp = k_{\perp r} + ik_{\perp i}$, where $k_{\perp i} \approx l(E)^{-1}$ [7]. In most materials, $l(E)$ is shortest, say only about 5Å or less, between $E = 20 \sim 150$eV[8]. From this viewpoint, some authors had argued that the ARPES should reflect only one-dimensional-density-of-states (ODDS) along a $k_\perp$ line for fixed $k_{//}$ in the Brillouin zone[9]. On the contrary, it has been shown that the ARPES results in many metals[10] and few semiconductors[11] can be interpreted well by the DTM. The most general expression to simulate this ambigous effect is seemed to formulate by a Lorentzian convolution of $k_\perp$ component as follows,

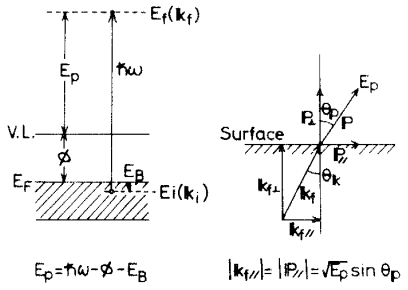

Fig.2. The energy conservation in the photoemission process and the relations between inner and outer momenta of photoelectron in the ARPES.

$$I(E_p,\vec{p},\vec{\varepsilon}) \sim \sum_{i,\vec{g}} \int_{BZ} d\vec{k}_\perp |M_i(\vec{k},\vec{\varepsilon})|^2 \delta[E_f(\vec{k}_f)-E_i(\vec{k}_i)-\hbar\omega]\,\delta(\vec{k}_{f//}-\vec{p}_{//}) \frac{\Gamma}{\Gamma^2+(k_\perp-k_{f\perp})^2}$$

$\vec{k}=\vec{k}_{f//}+\vec{k}_\perp$; $\vec{k}_f=\vec{k}_i+\vec{g}$; $\Gamma=1/l\cos\theta'$, θ' : inner polar angle

where $E_i(k_i)$ is the initial energy and $\vec{g}$ the reciprocal lattice vecter. The spectral dependences on the s and p polarizations of incident light are useful to identify the symmetries of initial states to be excited by a simple argument of the dipole selection rule in the optical transition[12], $M=\langle\psi_f|\vec{A}\cdot\vec{p}\,|\,\psi_i\rangle$, where ψ_i and ψ_f are initial- and final-state Bloch wave,functions respectively. Considering initial- and final-state momenta $\vec{k}_i$ and $\vec{k}_f$ lying in a mirror plane (MP) in the Brillouin zone, ψ_i and ψ_f must be either even or odd under reflection in that MP. The matrix element M is nonzero only if the integrand is even under the reflection. The photoelectron emitted in that MP is in a plane wave state at the detector, therefore ψ_f has even parity. The dipole operator $\vec{A}\cdot\vec{p}$ and ψ_i are of even parity if $\vec{A}$ is parallel to the MP and odd if $\vec{A}$ is perpendicular to the MP.

In this paper we report about our ARPES apparatus designed recently so as to make the various angle dependent measurements,mentioned above,possible in high precision. In §2, the design priciple is described and the layout of whole apparatus is given in §3. In §4, the main equipments installed in our apparatus are explained in detail and some typical results observed in practice are given as the examples showing the performance of the apparatus.

§2. Design Principle

The design principle is governed by following requirements for us.

1). It is desired to change the parameters α, $\hbar\omega$, $\vec{A}$, θ, ϕ and the index(hkl) of sample surface independently with one another.

2). The sample surface should be regulated well and be able to identify its physical and chemical situations before the ARPES experiment.

3). It must make possible to investigate both the clean and adsorbed surfaces.

On the first requirement, the photon energy $\hbar\omega$ depends completely on the kind of the light source used. As described in §1, the synchrotron radiation emitted from the storage ring is best at present, but the machine time allowed is limited in usual. Therefore, the UV light source of laboratory type is needed for the routine work. The direction of vector potential $\vec{A}$ of the incident light can be controlled in principle by a polarizer consisting of the mirror system, but the reflection efficiency is not high in general in vacuum UV range. Then the UV polarizer had no first priority in our case in view of the intensity gain. At the first stage of our design, the mechanical complication imposed us to limit the motion of electron analyser only within a horizontal plane, which means that the α and θ can vary only in the same plane though independently. The ϕ can be changed by a manipulation of the sample and the index(hkl) is set before the measurements.

The second requirement for our apparatus plays an essential role in the ARPES experiment. At first, a clean ultra-high vacuum better than 10^{-10}Torr at least is required in order to stabilize the surface situations as possible as long period. A differential pumping system has to be installed naturally

between the windowless discharge lamp as the light source and the UHV chamber in the case of laboratory work. The sample preparation equipments such as a cleaving device for single crystal, an ion-bombardment system for cleaning the surface and the cooling and heating assemblies for thermal regulations of the sample should be provided necessarily. Also the testing and checking devices for the surfaces after treatments are needed unavoidably. For examples, the Auger apparatus is important to check the surface cleanliness or purity with high sensitivity and the LEED, RMEED or RHEED apparatus is a requisite to determine the surface geometries.

The third requirement imposes us to build in the apparatus a gas-inlet system, which can be operated as our will under regulations of the pressures and purities of desired gases to be adsorbed on the sample surfaces.

§3. Layout in UHV Chamber

The structure and the arrangement of main comprising parts in our ARPES apparatus are schematically shown in Fig.3 for explanation. The treating, testing and checking devices for the sample surfaces are attached on the upper plane in UHV chamber and the ARPES measurement itself is performed in the lower plane. The sample manipulator is situated vertically on the top of the chamber. In the upper plane, the Ar^+ ion gun for bombarding the sample surfaces, the in situ cleaving device for some single crystals, the Auger apparatus and both the LEED and RHEED apparatuses are installed. In the lower plane, the assembly of electron analyser which can be rotated manually from outside the vacuum in situ with high precesion and the windowless discharge lamp equipped with the two-stage differential pumping system are installed. The gas inlet system can be attached somewhat arbitrary to one of manifolds remained in the chamber.

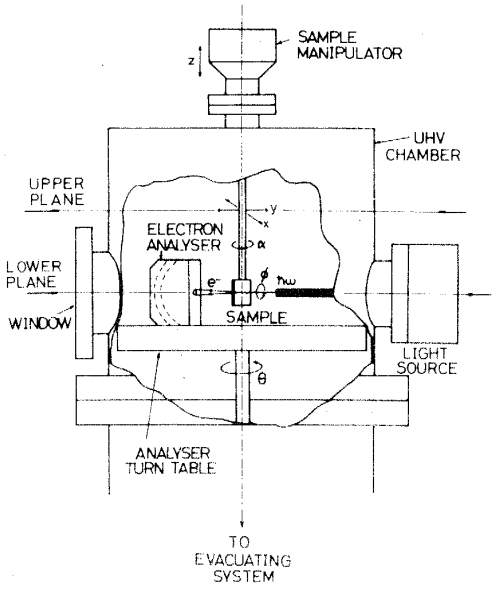

Fig.3. A layout in the main vacuum chamber of our ARPES apparatus.

The UHV chamber is evacuated by a 300^{l}/sec noble ion-pump, a 100^{l}/sec turbo-molecular pump, a Ti sublimation pump and a sorption pump. After one night baking, 5×10^{-11} Torr vaccum can be attained. The vacuum is calibrated by a nude ionization gauge and the residual gases are checked by a quadrupole mass-spectrometer.

§4. Detailed Descriptions of Main Devices

In this section the electron energy analyser, the light source assembly, the RHEED apparatus and the gas inlet system are explained in detail.

1). Electron Energy Analyser.

The electron energy analyser of a 150° spherical sector type is used, which is made from aluminum and has a 50mm mean radius of curvature. This was made in our laboratory. In this type of analyser, the kinetic energy E of electron passing through the analyser is related to the potential difference V_p between the inner- and outer-spherical electrodes and the radii of curvature R_1 and R_2 of the inner- and outer-electrodes, respectively, as follows,

$$eV_p = E(R_2/R_1 - R_1/R_2)$$

In our case, R_1 = 45mm and R_2 = 55mm, then eVp = 0.404E, the simple linear relation between V_p and E holds. Providing that various aberrations to be appeared in electron optics are negligible, the energy resolution is given by

$$E/\Delta E = 2R_0/\omega;\ R_0 = (R_1 + R_2)/2$$

where ω is a diameter of both the entrance and exit slits shaped into a circular aperture of same size. As ω = 1mm in our case, $E/\Delta E$ = 100, which was confirmed in practice by an electron beam of known energy experimentally. The distance between the sample to be situated in right position and the aperture is 30mm, which corresponds to a 1.9° full acceptance angle, and the analyser sees a circular area of 1mm diameter on the sample surface. The analyser is shielded from the external magnetic fields by an envelope made of μ-metal of 2mm thickness.

We have two scanning modes of operation of the analyser to observe the energy distribution curves of electrons. One mode is to scan the V_p under keeping both the slit and sample at the same constant potential, and the other is to scan the retarding voltage V_R between the slit and sample under fixing the V_p at a certain constant potential. We call the former scanning mode as the analyser or V_p scanning mode and the latter as the retarding or V_R mode for simplicity. As can be seen easily, the pass-energy of electrons through the analyser is maintained at certain constant value during the whole scanning time, in the retarding mode of operation. Therefore, the energy resolution is constant over the full energy range of spectra obtained, which is a desirable feature for the sake of analysis of the spectra though the intensity gain is lowered by retardation. On the other hand, a merit of employing the V_p scanning mode is at its higher intensity gain, but the varying energy resolution over a spectrum is a serious demerit. Selection of either mode in operations therefore depends on the purpose of measurement.

The photoelectrons passed through exit slit are detected by a channeltron, and the signal pulses are stored under control by the minicomputer through a preamplifier, a linear amplifier, a pulse height analyser, a timer and a scaler. The power supplies for V_p and V_R are regulated also by the minicomputer. All these detecting and data processing systems are the standard signal-counting techniques nowadays.

The analyser assembly is mounted on a turn table situated in UHV chamber, which can be rotated manually from the outside of vacuum in 360° angular range. In practice, however, a Pyrex-glass capillary tube used for the differential pumping system, about which is described in the next, limits the full rotation within about 300° angular range.

2). The Light Source Assembly

The light source is a capillary-discharge lamp as shown in Fig.4, which consists of a 5cm long quartz tube with a bore of 1.5mm diameter and

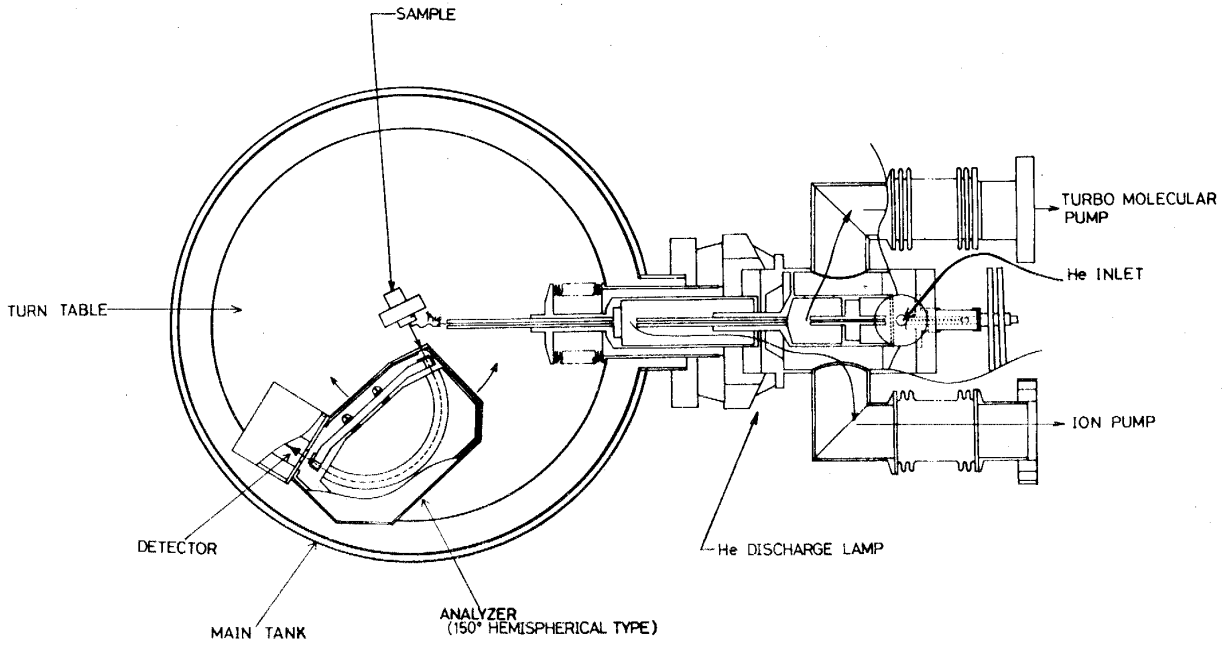

Fig. 4. A cross-section at the lower plane of the main UHV chamber

aluminum electrodes attached to the both ends of the tube. Usually the helium or neon gas is used as a discharge carrier. A stable operation during long period is possible under a typical power supply of 600V × 60mA and the optimum running pressure in the tube is nealy 0.10 Torr for HeI(21.2eV) and HeII(40.8eV) lines, 0.12Torr for NeI(16.8eV) and 0.08 Torr for NeII(26.8eV).

Since the suitable window materials to separate the vacuum into both sides of the light source and the UHV chamber are not obtainable in the Vacuum UV range, the two-stage differential pumping system has to be installed instead of the window. As shown in Fig. 4, the each stage is connected only by a Pyrex-glass capillary tube of a 1.0mm diameter, where the first stage is evacuated by a oil-diffusion pump with a liquid nitrogen trap or a turbo-molecular pump up to about 5×10^{-5}Torr and the second stage is by a noble ion-pump up to about 5×10^{-7}Torr. It is easy to maintain the $3 \sim 4 \times 10^{-10}$Torr vacuum in UHV chamber even under running operation of the He discharge.

Examples of the performances of the light source and electron energy analyser system are shown in Table 1 for the cases of Cu single crystal with (111) surface net plane as typical ones, where V_A is the accelerating voltage for photoelectrons and the maximum gain at V_R scanning mode in the 3d spectra is given at the lowest column. The higher gain can of course be obtained by using the thicker Pyrex-glass capillary tubes than above, with the expense of lower vacuum in the UHV chamber.

Table 1. Typical examples showing the performances of our electron analyser and light-source system. The cases at the V_R scanning mode for the photoemission from the Cu single crystal with clean (111) surface are shown, where the power supply for the discharge lamp is 600V × 60mA.

Resonance Line Used	NeI (16.8eV)	HeI (21.2eV)	NeII (16.8eV)	HeII (40.8eV)
V_p (eV)	7	10	15	25
V_A (V)	0	0	0	0
V_R (V)	0 ~ 8	0 ~ 9	2 ~ 11.2	4 ~ 14
Step.Voltage/channel(eV)	0.02	0.02	0.02	0.02
Energy Resolution,ΔE(eV)	0.07	0.10	0.15	0.25
Intensity gain(counts/sec)	1,500	2,500	6,000	1,300

3). The Sample Manipulators

The samples are attached rigidly on a holder plate at the lowest end of the manipulator. Three manipulators were prepared. Among them one was home made and two were made in Vacuum Generator. The latters have five degrees of freedom of motion for the fine adjustment of sample position and orientation, i. e., the translations along x and y axes in the horizontal plane and along vertical z-axis, and the rotations around about both the z axis and the surface normal of the sample. The rotation of the sample around the z axis makes possible to vary the incidence angle α of light in high precision and that around the surface normal axis makes possible to change the azimuthal direction of the sample in situ. The home-made manipulator has also the similar mechanisms as VG's ones except the rotation around sample normal, and the sample can be cooled down to a liquid nitrogen temperature. In one of the VG manipulators, the temperature of the sample can be regulated from a liquid nitrogen temperature up to about 700°C. In all cases, the up and down motions of the sample between the upper and lower planes in the UHV chamber can be achieved smoothly by a driving motor attached externally.

4). The RHEED Apparatus And Other Auxiliary Equipments

In order to see the microscopic geometies in the surface region of solids, the LEED or RHEED apparatus has to be used. In our case, both were installed,

where the RHEED could be used also as a RMEED. The LEED used is of a 4-grid type and has no special features different from conventional ones. On the contrary, the RHEED was extremely useful for our purpose though rather simple in its structure as shown in Fig.5 schematically. Our RHEED apparatus consist of an electron-gun assembly, a diaphragm slit to limit the beam aperture, a fine slit with a pin-hole of about a 0.15mm diameter to sort out an optimum beam position and also to confine the beam within a narraw cone, a coil to adjust the beam focussing and a small quadrupole magnet to deflect the beam into desired direction. The electrons can be accelerated up to about 30kV and the incident beam upon the sample with a grazing angle to the surface irradiates a surface area of about a 0.5mm diameter. The RHEED or RMEED patterns thus obtained can be seen directly on a fluorescent screen just behind a viewing port situated on the opposite side from the gun assembly in the UHV chamber. A Cu(111) 1×1 RHEED pattern obtained by the 10keV incident electron beam is shown in Fig.6 as an example, where the beam is incident along the $[1\bar{1}0]$ direction of the sample surface under 10^{-11}Torr vacuum. The five vertical lines as seen clearly on the screen arrange regularly with equal distance, which are due to the Bragg reflections by the rods in the reciprocal lattice plane corresponding to the Cu(111) surface net plane having a 1×1 structure, and a few crossing curves also seen in Fig.6 are the Kikuchi patterns. The RHEED pattern can be utilized to identify the azimuthal direction of sample surface. By our experiences, the RHEED is more advantageous for our ARPES measurements than the LEED in its simpler electron optics, easier recognition of the patterns and wider space allowance for the measurements, at least in the cases of clean surfaces.

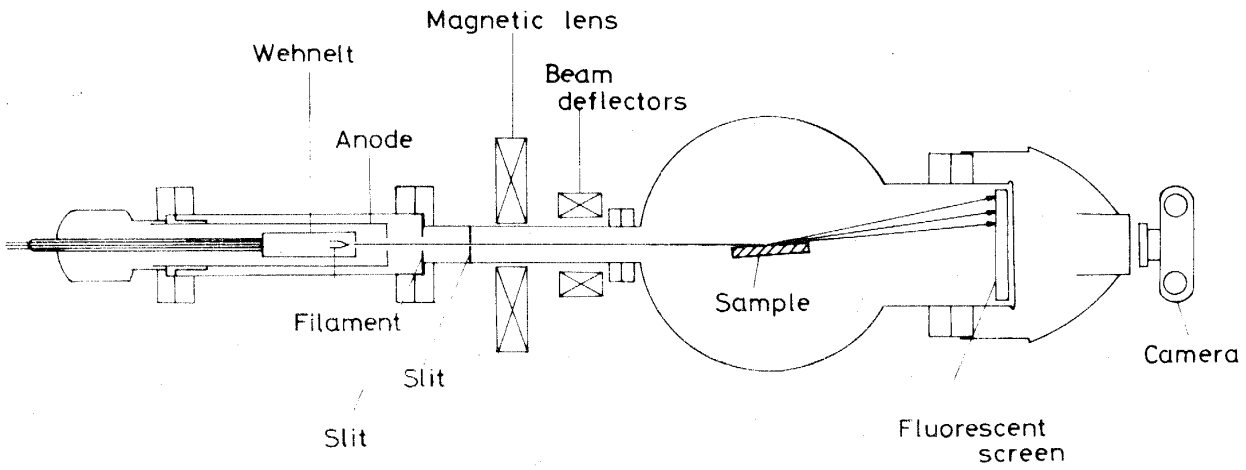

Fig.5. Schematic structure of our RHEED equipment.

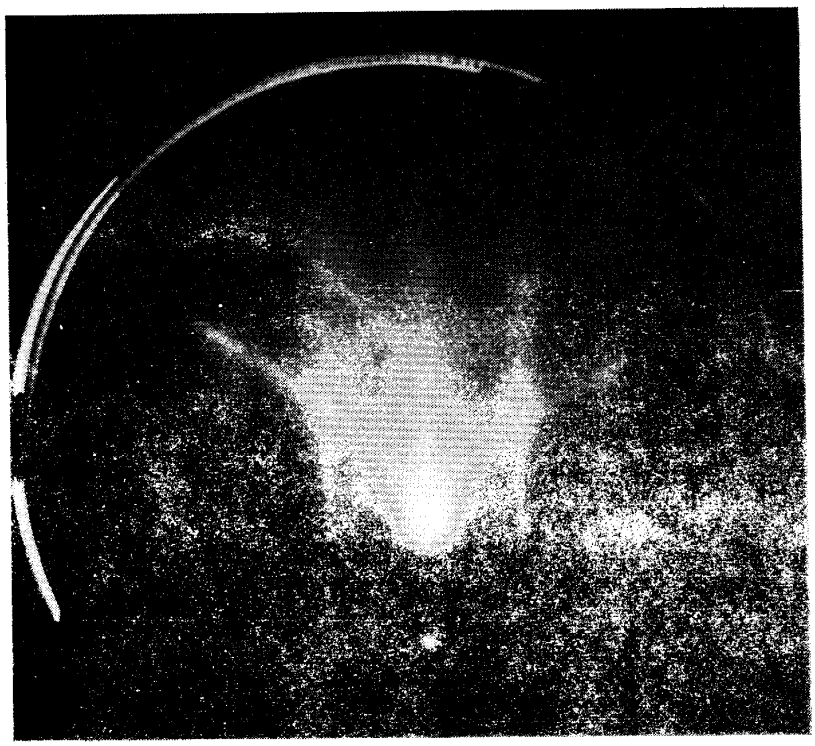

Fig. 6. An example of obtained RHEED patterns. The case where 10keV electrons is incident upon the Cu (111) face along [1$\bar{1}$0] axis is shown.

It is well-known that the Auger spectra excited by moderately low energy electrons are useful to examine the surface cleanliness. This is also the case in our apparatus and the PHI's equipment is installed.

A quadrupole mass-spectrometer is attached to one of manifolds of the UHV chamber in order to check the residual gas components, which can analyse the mass number up to 300.

5) The Gas-Inlet System

In the studies of adsorbed surface, one of the most important things to be noted is of course to prepare the well-regulated surfaces at an initial stage of the investigation. Therefore, the gas inlet system has a key importance in the ARPES measurements of the adsorbed systems. Our gas inlet system designed on this viewpoint is shown by a diagram in Fig.7, which can also be served as a rare-gas supply for the discharge lamp. The gases to be adsorbed on a clean surface of the sample are prepared previously as purely as possible, which are stored in glass cylinders usually and attached to the valves V13 ~ V15 shown on top right in Fig.7. The desired gas is stored in the next within a 5 ℓ reservoir through a variable-leakage valve V12 and then a known quantity of the gas is inlet into the UHV chamber through the valves V11 and V2. After finishing the exposure of gas to the sample, the chamber is evacuated by an alternation of two ways, i. e., the one the line passing through an ion-pump IP(1) and a getter pump GP(1) and the other the line through a turbo-molecular-pump TMP and a rotary pump RP(1). The cylinder for rare-gas supply to the discharge lamp is attached to a leakage valve LV4 and the gas is inlet into the lamp through a line along a V18, a sorption pump SP, a V17, a 5 ℓ gas reservoir and a variable-leakage valve APC(automatic pressure control). The used rare-gas after discharge is evacuated continuously through the TMP and RP(1) line, where the leakage unit shown in bottom right in Fig.7 is for a

protection of TMP from the emergent stops of electric power and water supplies. In Fig.7, the notations IG and PG mean the ionization and Pirani gauges, respectively.

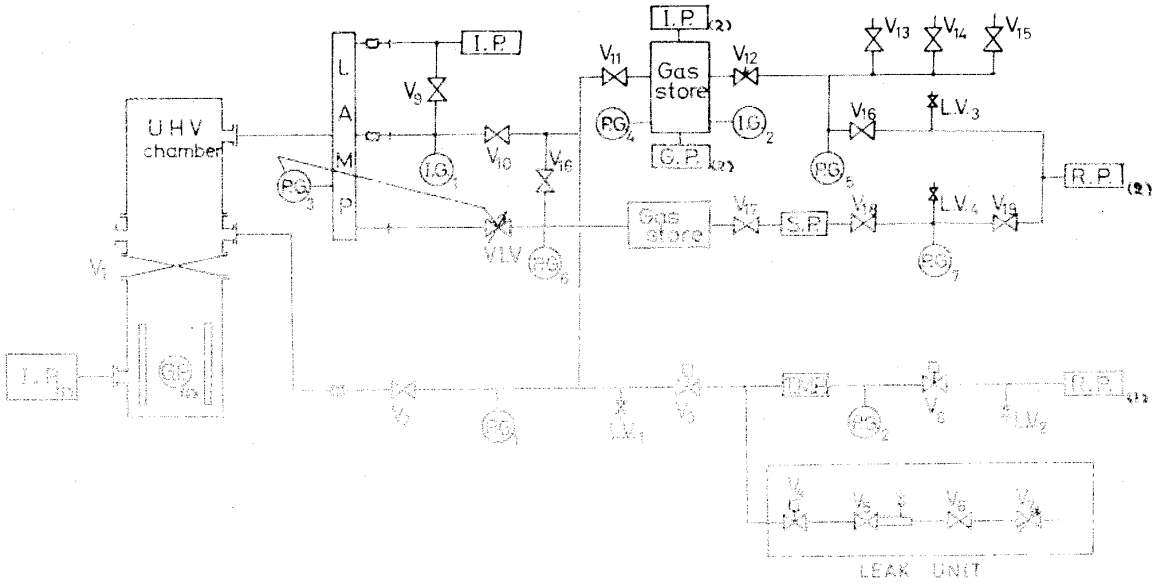

Fig.7. A block-diagram of our gas-inlet system.

§5. Some Typical Results Showing The Performance Of Our ARPES Apparatus.

Untill recently, various ARPES measurements were performed already by our ARPES apparatus. Especially the polar-angle-dependent spectra of Cu single crystal with (111)surface were obtained throughly from $\theta = -20°$ to $+70°$ within three azimuthal planes corresponding to the ΓLKL, ΓLUK and ΓLWK planes in the Brillouin zone, the results of which will be published partly elsewhere[13]. Similar measurements are going on the Cu crystals with (110) and (100) surfaces and on the Ni crystals with (111),(110) and (100) surfaces. The ARPES of Si crystals with (111) surfaces having both the 2 × 1 structure cleaved in situ and the 7 × 7 structure were observed. The apparatus was tested also by the synchrotron radiation emitted from the SOR-Ring at the Synchrotron Radiation Laboratory, Institute of Solid State Physics, University of Tokyo during the four weeks machine time given for us. At that time the $\hbar\omega$ dependent ARPES between about 40 and 150eV were observed mainly for the Cu and Europium hexaborides. In this paper, only a few typical results are shown to demonstrate the performances of our apparatus.

1). The Polar-Angle Dependences Of Cu(111) And Ni(111) Spectra

In Fig.8, the polar-angle dependences of Cu(111) and Ni(111) spectra are shown for comparison with each other, where the data excited by HeI(21.2eV) resonance line incident upon the surface at 45° angle were obtained within the

ΓLKL azimuthal plane in both cases. These data are only a part of the massive results obtained in practice untill now. In the case of Cu, many sharp structures appear in the spectra in constrast with the case of Ni as seen in Fig.8. The former apporves the high resolution in our apparatus and the latter is mainly due to the short lifetime of hole states[14].

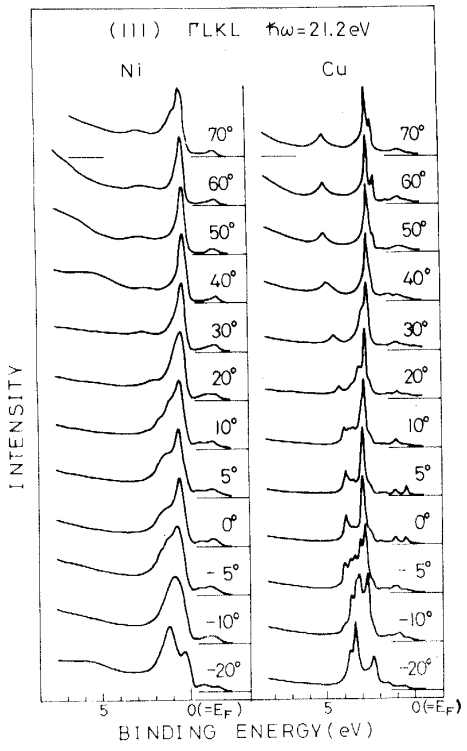

Fig.8. The polar-angle(θ) dependent ARPES of Ni(111) (left) and Cu(111) (right) within ΓLKL azimuthal plane from θ=-20°to+70°, where HeI resonance line was used at a 45° incidence angle.

In Fig. 9, the very sharp peak due to d-like surface states of Cu with (111) surface are shown, which appears at about 2eV initial energy between θ = 35° ~ 70° in the spectra observed within the ΓLUK plane. The case of the clean surface excited by HeI(21.2eV) excitation and observed at θ = 60° is shown as an example on the bottom of Fig.8. The upper curve shows the spectrum under same condition as in the lower curve but after O_2 exposure of about 500L, where the sharp peak disappears completely as shown in expanded scale on top right. Surprisingly, the width of the surface state peak in Fig.8 is only about 0.1eV or less and nearly equal to our energy resolution 0.1eV shown in Table 1, which means an intrinsic width of surface state of a few ten meV.

2). The Normal Emissions In Si (111) With Cleaved 2 × 1 Surface Structure.

It is known that the Si(111) surface cleaved in situ is most clean and has the 2 × 1 structure. We have tried repeatedly to observe the reproducible ARPES of cleaved Si(111). As the result it was found that the spectrum changes its profile dependent upon the spending time after cleavage in situ even in UHV of the order of 10^{-11}Torr and also upon the vacuum at cleaving time. Fig.10 shows the one of results in normal emission obtained from the (111) cleaved surface in 5×10^{-11}Torr vacuum, where the spending time after the cleavage is shown on the right of each curve. In the bottom curve for example, the measurement starts at 10 minutes after the cleavage and needs about 20 minutes to complete the curve. A sharp peak appeared at 0.8eV initial energy is due to the filled dangling-bond surface state as known well and the back-bond surface states contribute to the broad band from 1.5eV to 5eV. Intensity of the dangling-bond surface state decreases rather rapidly with time and becomes to only a step-like shoulder after 12 hours. On the contrary, a broad band appeared around at about 7.5eV is very low at an initial stage but grows up with time, which may be due to oxygen contaminations from the viewpoint of its energy position

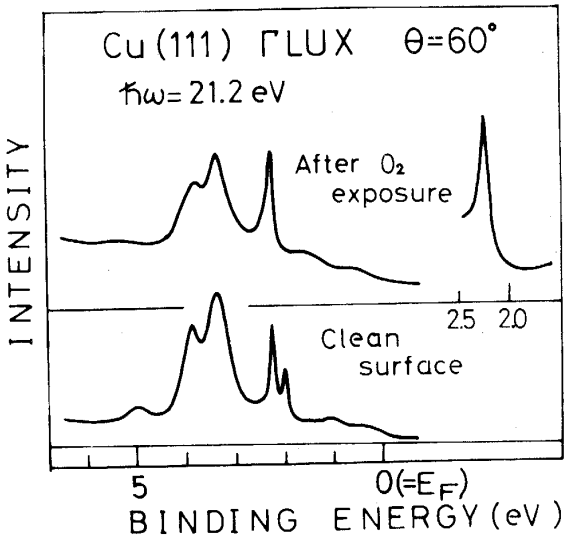

Fig.9. The ARPES at θ=60° within ΓLUX plane of the clean(lower) and 500L O_2 exposed(upper)Cu(111) surfaces, where HeI resonance line was used at a 45° incidence angle. A sharp peak appeared at about 2eV initial energy on the lower is due to the d-like surface state and disappears on the upper.

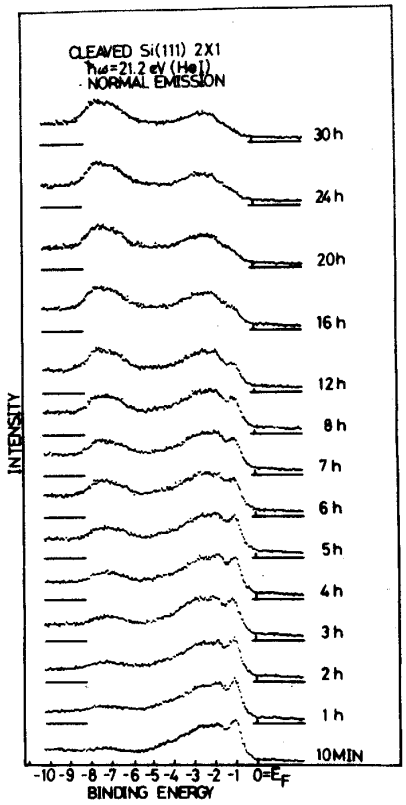

Fig.10. Time dependent changes in the spectral profiles of Si(111) 2×1 ARPES at normal emission after cleaving the sample, where the time spended is shown on the right of each curve. HeI resonance line was used.

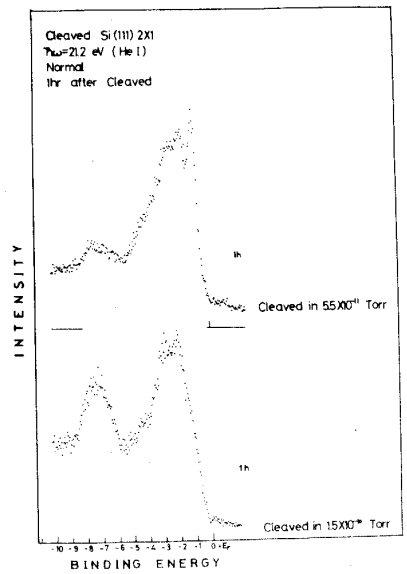

Fig.11. The normal emission profiles of Si(111)2×1 ARPES obtained at 1 hour after cleaving the sample in different vacuum conditions. The upper profile is for the sample surface cleaved at 5.5×10^{-11} Torr and the lower for the surface at 1.5×10^{-10} Torr.

though not detected by Auger spectra. As seen in Fig.10, the spectral profile changes rather seriously from the initial one only after four hours. Thus it is known that the ARPES of cleaved Si(111) have to be observed within two hours

at least after cleavage even in 5×10^{-11}Torr vacuum. In Fig.11, two spectral profiles of ARPES of Si(111) at 1 hour after cleaving the sample within different two vacua are shown for comparison, where the uppor curve is for the sample cleaved in 5.5×10^{-11}Torr vacuum and the lower in 1.5×10^{-10}Torr. The dangling-bond surface-state peak at 0.8eV is seen only as a weak shoulder in the lower curve. These results suggest that further careful ARPES measurements have to be done repeatedly in order to obtain a reliable and reproducible result in such cases as in silicon sample.

§6. Acknowledgements

The authors would like to acknowledge Dr. S.Ino in the Research Institute for Iron, Steel and Other Metals, Tohoku University for his kind advices to the construction of our RHEED apparatus. Thanks are also due to Dr. T.Kobayasi in College of Medical Sciences, Tohoku University, for his invaluable discussions in the analysis of the results. The present work was supported mainly by the Grant-in-Aid from the Ministry of Education and partly by the Mitsubishi Science Foundation.

References

1) See, for example, B.Feuerbacher, B.Fitton and R.F.Willis: Photoemission and the Electronic Properties of Surfaces (John Wiley & Sons, New York, 1978), and references therein.

2) See, for examples, M.Cardona and L.Ley: Photoemission in Solids I (Spinger-Verlag, Berlin, 1978).
L.Ley and M.Cardona: ibid II and references therein.

3) W.Eib and S.F.Alvarado: Phys. Rev. Letters, 37(1976) 444.
S.F.Alvarado, W.Eib, F.Meier, H.C.Siegmann and P.Zürcher:Photoemission of Spin Polariged Electrons, chap. 15 in ref.1.
I.D.Moore and J.B.Pendry: J.Phys.,C11(1978) 4615.
N.V.Smith and S.Chiang: Phys. Rev., B19(1979)5013.

4) See, for example, C.Kunz: Synchrotron Radiation as a Source for Photoemission, chap. 17 in ref.1.

5) S.Kono, G.S.Fadley, N.F.T.Hall and Z.Hussain: Phys. Rev. Letters, 41(1978) 117.

6) C.H.Li and S.Y.Tong: Phys. Rev. B19(1979)1769.

7) P.J.Feibelman and D.E.Eastman: Phys. Rev., B10(1974)4932.

8) W.E.Spicer: Vacuum Ultraviolet Radiation Physics ed. by E.E.Koch, R.Haenzel and C.Kung (Vieweg - Pergamon, Braunschweig, 1974) P.545.

9) T.Grandke, L.Ley and M.Cardona: Phys. Rev.Letters, 38(1977)1033.
L.Ley, M.Cardona and R.A.Pollak: Photoemission in Semiconductors, chap.2 in ref. 2, II.

10) D.Liebowitz, M.Sagurton, J.Colbert and N.J.Shevchik: Phys. Rev. Letters, 39(1977)1625.
J.Stöhr, P.S.Wehner, R.S.Williams, G.Apai and D.A.Shirley: Phys. Rev., B17(1978)587.
G.V.Hansson and S.A. Flodström: Phys. Rev., B17(1978)473.
S.P.Weeks: Phys. Rev.,B17(1978)1738.
K.Furusawa, S.Suzuki, T.Sagawa and T.Kobayasi: Proc.Int.Conf. X-Ray & XUV Spectroscopy, Sendai, 1978, Jpn. J.Appl. Phys., 17(1978) Suppl. 17-2,p.255.
D.E.Eastman, J.A.Knapp and F.J.Himpsel: Phys. Rev. Letters, 41(1978)825.
P.Thiry, D.Chandesris, J.Lecante, C.Guillot, R.Pinchaux and Y.Pétroff: Phys. Rev. Letters, 43(1979)82.
11) T.C.Chiang, J.A.Knapp, D.E.Eastman and M.Aono: Solid State Commun. (in Press).
12) G.W.Gobeli, F.G.Allen and E.O.Kane: Phys. Rev. Letters, 12(1964)94.
J.Hermanson: Solid State Commun., 22(1977)9.
13) K.Furusawa, M.Yoshida, S.Suzuki, T.Kobayasi and T.Sagawa: to be published.
14) J.B.Pendry: Electron Emission from Solids, chap. 4 in ref.1.